

Three-Level Optimized Pulse Patterns with Eliminated Torque Harmonics

Isavella Koukoula

Faculty of Inf. Technol. and Commun. Sciences
Tampere University
Tampere, Finland
isavella.koukoula@tuni.fi

Petros Karamanakos

Faculty of Inf. Technol. and Commun. Sciences
Tampere University
Tampere, Finland
p.karamanakos@ieee.org

Tobias Geyer

Motion System Drives
ABB Switzerland
Turgi, Switzerland
t.geyer@ieee.org

Abstract—This paper presents the computation of three-level optimized pulse patterns (OPPs) that minimize, and, when physically possible, eliminate the low-order torque harmonics by incorporating explicit constraints into the optimization problem. To prevent the consequent deterioration in the output current quality, the symmetry constraints typically imposed on OPPs are relaxed. As a result, the proposed OPPs not only suppress the targeted torque harmonics but also keep the current harmonics low and close to those of conventional OPPs, as demonstrated by the presented numerical results. At the same time, the torque ripple produced by the proposed OPPs is comparable to—or, for some modulation indices, even lower than—that of conventional programmed modulation methods.

Index Terms—Medium-voltage (MV) drives, pulse width modulation (PWM), optimized pulse patterns (OPPs), torque harmonics, current harmonics.

I. INTRODUCTION

In pulse width modulated (PWM) converters, the switching nature of the generated output voltage introduces harmonic distortions in the output current. Conventional PWM methods, such as carrier-based PWM (CB-PWM) and space vector modulation (SVM), can produce currents of high quality when the switching-to-fundamental frequency ratio, i.e., the pulse number, is high. However, in medium-voltage (MV) drives, where the switching frequency is kept low to limit the switching losses, their performance significantly deteriorates. Therefore, programmed PWM methods such as selective harmonic elimination (SHE) [1], [2] and optimized pulse patterns (OPPs) [3] offer a favorable approach for achieving minimal harmonic distortions at low pulse numbers.

Regardless of the PWM method used, harmonic distortions appear in the stator flux and current. The interaction between these two physical quantities results in low-order torque harmonics. These harmonics are undesirable because, when their frequencies are close to the mechanical resonance of the shaft, they can lead to pulsating torque oscillations and potentially damage the motor shaft [4], [5]. Therefore, it is desirable to minimize the amplitude of these harmonics, if not eliminate them entirely.

These low-order torque harmonics can be mitigated at the control level by generating the appropriate current reference to compensate for them [6], [7]. However, it can be beneficial to account for them in the modulation stage to keep the control

structure simple. In this direction, [8] proposed a modified SVM method that combines discontinuous and continuous switching patterns with different switching frequencies. Moreover, by adjusting the carrier frequency of the hybrid discontinuous PWM patterns, the torque ripple can be reduced while simultaneously lowering the switching losses [9]. These methods, however, are designed for high pulse numbers, and their operating principles may no longer hold when the pulse number is significantly reduced.

For low pulse numbers, programmed PWM methods are generally preferred. For example, SHE eliminates a predefined number of low-order current harmonics for a given pulse number, effectively reducing the total demand distortion (TDD) of the output current compared to conventional PWM methods operating at the same switching frequency. As a byproduct, since the low-order current harmonics are zero, the resulting low-order torque harmonics are also eliminated. However, the utilization of the dc-link voltage is limited because it is not possible to eliminate the low-order current harmonics over the whole modulation range. On the other hand, conventional OPPs are computed through an offline optimization procedure that minimizes the stator current TDD, thus achieving the lowest harmonic distortions for a given pulse number. However, they do not directly reduce the low-order current harmonics, which contribute to low-order torque harmonics [10]. Hence, although these harmonics are usually lower than with conventional PWM methods, their amplitudes are not explicitly addressed during the OPP design process.

To suppress the vibrations and noise caused by torque harmonics, [11] and [12] proposed the computation of OPPs that minimize the torque—instead of the current—TDD. Moreover, by including additional constraints that relate to the amplitude of the OPP harmonics, individual torque harmonics can be eliminated [13]–[15]. However, such an approach increases the harmonics at higher frequencies, thus deteriorating the current quality. Furthermore, the modulation range over which the low-order torque harmonics can be eliminated is limited. To tackle this issue and compute OPPs at high modulation indices, [16] proposed minimizing the current TDD while keeping the torque harmonics within predefined limits. Alternatively, the current harmonics that give rise to low-order torque harmonics can be bounded, as shown in [17] for

interior permanent magnet synchronous motors (IPMSMs), albeit without eliminating them. Moreover, to achieve a good balance between current and torque quality, the two objectives can be combined into a single objective function, as shown in [18] and [19] for dual three-phase PMSMs (DTP-PMSMs).

As shown in [20], by relaxing the symmetry properties of the pulse pattern, not only the amplitude but also the phase of the current harmonics can be manipulated, introducing additional degrees of freedom into the optimization problem. This feature can be exploited to improve the current harmonic performance while eliminating targeted torque harmonics. In addition, due to the relaxation of the OPP symmetry, the modulation range for which the torque harmonics can be eliminated is increased. Hence, the limitations of the aforementioned programmed PWM approaches can be overcome by appropriately designing the OPP optimization problem.

Thus, this paper proposes the computation of OPPs with relaxed symmetry properties that eliminate the low-order torque harmonics. As a first step, an analytical relationship between the OPP harmonics and resulting torque harmonics is derived. This is used to directly constrain the low-order torque harmonics in the OPP problem. Additionally, as shown, the relaxation of the symmetry properties effectively enables the elimination of the low-order torque harmonics for the widest possible range of modulation indices without significantly compromising the current quality. When complete elimination is not physically possible, OPPs with limited torque harmonics are computed up to the maximum achievable modulation index. The presented numerical results based on an MV drive consisting of a three-level neutral-point-clamped (NPC) converter and an induction machine (IM) demonstrate the benefits of the proposed approach.

II. CONVENTIONAL THREE-LEVEL OPPS

Consider a three-level 2π -periodic switching pattern $u(\theta)$ with fundamental frequency f_1 and $4d$ switching events, i.e., transitions, per fundamental period, where d is the pulse number. This implies that the resulting device switching frequency is $f_{sw} = df_1$. Each of these switching transitions $\Delta u_i = u_i - u_{i-1} \in \{-1, 1\}$, with $i \in \{1, \dots, 4d\}$, and switch positions $u_j \in \{-1, 0, 1\}$, $j \in \{0, \dots, 4d\}$, occurs at a switching angle α_i .

Due to the 2π -periodicity, the pulse pattern can be described by the Fourier series

$$u(\theta) = \frac{a_0}{2} + \sum_{n=1}^{\infty} (a_n \cos(n\theta) + b_n \sin(n\theta)), \quad (1)$$

where a_n and b_n are the Fourier coefficients of the n^{th} switching harmonic. The corresponding voltage harmonics are given by

$$v_n = \frac{V_{dc}}{2} u_n, \quad (2)$$

where V_{dc} is the dc-link voltage. Based on the harmonic model of the machine shown in Fig. 1, it holds that

$$v_n = R_s i_n + X_\sigma \frac{di_n}{dt}, \quad (3)$$

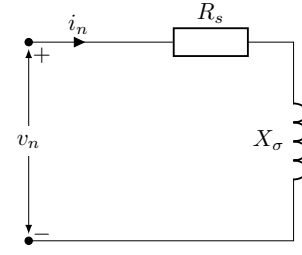


Fig. 1: Harmonic model of an induction machine

where X_σ denotes the total leakage reactance and R_s the stator resistance. Assuming that $R_s \approx 0$, the amplitude of the n^{th} current harmonic is

$$\hat{i}_n = \frac{1}{n\omega_1 X_\sigma} \frac{V_{dc}}{2} \hat{u}_n, \quad (4)$$

where ω_1 is the fundamental angular frequency and $\hat{u}_n = \sqrt{a_n^2 + b_n^2}$ is the amplitude of the n^{th} switching harmonic. Therefore, the load current TDD is given by

$$I_{\text{TDD}} = \frac{1}{\sqrt{2} I_{\text{nom}} \omega_1 X_\sigma} \frac{V_{dc}}{2} \sqrt{\sum_{n \neq 1} \left(\frac{\hat{u}_n}{n} \right)^2}, \quad (5)$$

where I_{nom} is the nominal current. Note that it can be deduced from (5) that the current TDD is proportional to the weighted sum of the harmonics of the switching signal.

The switching pattern (i.e., OPP) that produces the lowest possible harmonic distortions is computed by minimizing the load current TDD I_{TDD} . For conventional OPPs, three-phase and quarter- and half-wave symmetry (QaHWS) is assumed. Therefore, only d switching angles $\alpha \equiv \alpha_Q = [\alpha_1 \alpha_2 \dots \alpha_d]^T \in [0, \pi/2]^d$ are required to fully describe $u(\theta)$. Additionally, due to the QaHWS, the a_n Fourier coefficients are zero, while the b_n coefficients are

$$b_n = \frac{4}{n\pi} \sum_{i=1}^d \Delta u_i \cos(n\alpha_i), \quad n = 1, 3, 5, \dots$$

As a result, conventional QaHWS OPPs are computed by solving an optimization problem of the form

$$\begin{aligned} & \underset{\alpha_Q}{\text{minimize}} && J(\alpha_Q) = \sum_{n=5,7,\dots} \left(\frac{b_n}{n} \right)^2 \\ & \text{subject to} && b_1 = m \\ & && 0 \leq \alpha_1 < \alpha_2 < \dots < \alpha_d \leq \frac{\pi}{2}, \end{aligned} \quad (6)$$

where $m \in [0, 4/\pi]$ is the desired modulation index. Note that even harmonics are zero due to the QaHWS, while triplen harmonics do not drive harmonic current.

III. TORQUE-CONSTRAINED THREE-LEVEL OPPS

A. Torque Harmonics Modeling

A three-level NPC converter with an IM is shown in Fig. 2. The per unit (p.u.) electromagnetic torque of the IM is given by

$$T_e = \frac{1}{\text{pf}} (\psi_{s,\alpha\beta} \times i_{s,\alpha\beta}), \quad (7)$$

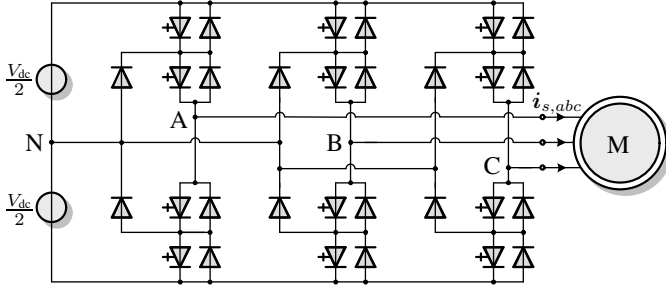


Fig. 2: Three-level NPC converter driving a machine.

where $\text{pf} = \cos \phi$ is the power factor, with ϕ being the displacement angle. Moreover, $\psi_{s,\alpha\beta}$ and $i_{s,\alpha\beta}$ are the stator flux and current, respectively, in the stationary $\alpha\beta$ -plane. These quantities can be expressed as the sum of their fundamental and harmonic components. Regarding the fundamental components, a fully magnetized machine is assumed, implying a flux amplitude $\Psi_s = 1$ p.u., while the amplitude of the current is denoted as I_1 .

The harmonic components of the flux and current can be computed based on the switching signal harmonics. To this end, the OPP switching signal is first transformed in the stationary $\alpha\beta$ -plane, resulting in

$$u_{s,\alpha} = m \sin \omega_1 t + \sum_{n=6k\pm 1} a_n \cos n\omega_1 t + b_n \sin n\omega_1 t \quad (8a)$$

$$u_{s,\beta} = -m \cos \omega_1 t + \sum_{n=6k-1} -a_n \sin n\omega_1 t + b_n \cos n\omega_1 t + \sum_{n=6k+1} a_n \sin n\omega_1 t - b_n \cos n\omega_1 t. \quad (8b)$$

Hence, with (8), (2), and the voltage equation

$$\mathbf{v}_{s,\alpha\beta} = R_s \mathbf{i}_{s,\alpha\beta} + \frac{d\psi_{s,\alpha\beta}}{dt}, \quad (9)$$

the stator flux can be written as (assuming $R_s \approx 0$)

$$\begin{aligned} \psi_{s,\alpha} &= -\Psi_s \cos \omega_1 t \\ &+ \sum_{n=6k\pm 1} -\frac{b_n}{n\omega_1} \frac{V_{dc}}{2} \cos n\omega_1 t + \frac{a_n}{n\omega_1} \frac{V_{dc}}{2} \sin n\omega_1 t \end{aligned} \quad (10a)$$

$$\begin{aligned} \psi_{s,\beta} &= -\Psi_s \sin \omega_1 t \\ &+ \sum_{n=6k-1} \frac{b_n}{n\omega_1} \frac{V_{dc}}{2} \sin n\omega_1 t + \frac{a_n}{n\omega_1} \frac{V_{dc}}{2} \cos n\omega_1 t \\ &+ \sum_{n=6k+1} -\frac{b_n}{n\omega_1} \frac{V_{dc}}{2} \sin n\omega_1 t - \frac{a_n}{n\omega_1} \frac{V_{dc}}{2} \cos n\omega_1 t. \end{aligned} \quad (10b)$$

with $k \in \mathbb{N}^+$.

The stator current harmonics can be derived with the help of (3). Therefore, the stator current can be expressed as a function of the OPP Fourier coefficients a_n and b_n as follows

$$\begin{aligned} i_{s,\alpha} &= I_1 \sin(\omega_1 t - \phi) \\ &+ \sum_{n=6k\pm 1} -\frac{b_n}{n\omega_1 X_\sigma} \frac{V_{dc}}{2} \cos n\omega_1 t + \frac{a_n}{n\omega_1 X_\sigma} \frac{V_{dc}}{2} \sin n\omega_1 t \end{aligned} \quad (11a)$$

$$\begin{aligned} i_{s,\beta} &= -I_1 \cos(\omega_1 t - \phi) \\ &+ \sum_{n=6k-1} \frac{b_n}{n\omega_1 X_\sigma} \frac{V_{dc}}{2} \sin n\omega_1 t + \frac{a_n}{n\omega_1 X_\sigma} \frac{V_{dc}}{2} \cos n\omega_1 t \\ &+ \sum_{n=6k+1} -\frac{b_n}{n\omega_1 X_\sigma} \frac{V_{dc}}{2} \sin n\omega_1 t - \frac{a_n}{n\omega_1 X_\sigma} \frac{V_{dc}}{2} \cos n\omega_1 t. \end{aligned} \quad (11b)$$

By substituting (10) and (11) into (7), the resulting non-zero torque harmonics are of order $n = 6k$, $k \in \mathbb{N}^+$, and can be written as

$$\begin{aligned} T_{e,n} &= \frac{V_{dc}}{2\omega_1 \text{pf}} \left(\left(\left(I_1 \sin \phi - \frac{1}{X_\sigma} \right) \left(\frac{b_{n-1}}{n-1} - \frac{b_{n+1}}{n+1} \right) - \right. \right. \\ &I_1 \cos \phi \left(\frac{a_{n-1}}{n-1} + \frac{a_{n+1}}{n+1} \right) \left. \right)^2 + \\ &\left(\left(I_1 \sin \phi - \frac{1}{X_\sigma} \right) \left(\frac{a_{n-1}}{n-1} - \frac{a_{n+1}}{n+1} \right) + \right. \\ &I_1 \cos \phi \left(\frac{b_{n-1}}{n-1} + \frac{b_{n+1}}{n+1} \right) \left. \right)^2 \left. \right)^{\frac{1}{2}}. \end{aligned} \quad (12)$$

Note that (12) can be further simplified under QaHWS conditions, as the coefficients a_n are zero.

B. OPPs That Eliminate/Minimize Torque Harmonics

To prevent mechanical oscillations, the 6th and 12th torque harmonics must be eliminated. To achieve this, the constraints

$$T_{e,6} = 0 \quad \text{and} \quad T_{e,12} = 0, \quad (13)$$

are added to problem (6). Due to the QaHWS, only the amplitude of the current harmonics can be manipulated. As shown in the appendix, this implies that achieving $T_{e,6k} = 0$ necessitates the elimination of both i_{6k-1} and i_{6k+1} . To avoid numerical issues caused by the hard constraints (13), and thus guarantee the feasibility of the torque-constrained OPP optimization problem even at high modulation indices, the equality constraints (13) are relaxed, and implemented as soft constraints of the form

$$T_{e,6k} \leq \epsilon_k, \quad k \in \{1, 2\}, \quad (14)$$

where ϵ_k is a slack variable introduced into the optimization problem. Thus, with (14), the proposed OPP problem is formulated as

$$\begin{aligned} \text{minimize}_{\alpha_Q, \epsilon} \quad & J(\alpha_Q) = \sum_{n=5,7,\dots} \left(\frac{b_n}{n} \right)^2 + \epsilon^T \mathbf{W} \epsilon \\ \text{subject to} \quad & b_1 = m \\ & 0 \leq \alpha_1 < \alpha_2 < \dots < \alpha_d \leq \frac{\pi}{2} \\ & T_{e,6k} \leq \epsilon_k, \\ & \epsilon_k \geq 0, \quad k \in \{1, 2\}, \end{aligned} \quad (15)$$

where $\epsilon = [\epsilon_1 \ \epsilon_2]^T$ is the vector of slack variables. Note that the slack variables are heavily penalized through the (diagonal) weighting matrix \mathbf{W} in the objective function to ensure that violations of the soft constraints are avoided whenever physically possible.

Eliminating specific low-order current harmonics, however, occurs at the cost of increasing the other harmonics at higher frequencies, which in turn increases the current TDD. To mitigate this, the symmetry of the OPP should be relaxed to half-wave symmetry (HWS). By doing so, both the amplitude and phase of the current harmonics can be manipulated. As a result, eliminating $T_{e,6k}$ only requires that i_{6k-1} and i_{6k+1} have equal (non-zero) amplitudes and a specific phase difference, as shown in the appendix. These additional degrees of freedom enable the elimination of low-order torque harmonics without significantly deteriorating I_{TDD} , as demonstrated in Section IV. Moreover, the same section shows that the relaxation of the symmetry increases the range of modulation indices over which the torque harmonics can be fully eliminated. Nonetheless, also in this case, soft constraints are preferred over hard constraints to avoid any feasibility issues.

Given the above, the proposed optimization problem for torque-constrained HWS OPPs is

$$\begin{aligned}
 & \underset{\alpha_H, \epsilon}{\text{minimize}} && J(\alpha_H) = \sum_{n=5,7,11,\dots} \frac{a_n^2 + b_n^2}{n^2} + \epsilon^T \mathbf{W} \epsilon \\
 & \text{subject to} && a_1 = 0, \\
 & && b_1 = m \\
 & && 0 \leq \alpha_1 < \alpha_2 < \dots < \alpha_{2d} \leq \pi \\
 & && T_{e,6k} \leq \epsilon_k, \\
 & && \epsilon_k \geq 0, \quad k \in \{1, 2\},
 \end{aligned} \tag{16}$$

where $\alpha_H = [\alpha_1 \ \alpha_2 \ \dots \ \alpha_{2d}]^T$ is the vector of the to-be-computed $2d$ switching angles due to the imposed HWS. Note that, as in problem (6), only odd non-triplen harmonics are considered since even harmonics remain zero due to the HWS. Moreover, $a_1 = 0$ such that the phase of the fundamental component is zero. Note that the Fourier coefficients of the HWS switching pattern are

$$\begin{aligned}
 a_n &= -\frac{2}{n\pi} \sum_{i=1}^{2d} \Delta u_i \sin(n\alpha_i), \quad n = 1, 3, 5, \dots \\
 b_n &= \frac{2}{n\pi} \sum_{i=1}^{2d} \Delta u_i \cos(n\alpha_i), \quad n = 1, 3, 5, \dots
 \end{aligned}$$

IV. NUMERICAL RESULTS

This section shows the optimization results for (a) conventional QaHWS OPPs (see problem (6)), (b) torque-constrained QaHWS OPPs (see problem (15)), (c) torque-constrained HWS OPPs (see problem (16)), and (d) SHE. OPPs in the ‘‘b’’ category are hereafter referred to as QaHWS–T OPPs, and those in category ‘‘c’’ as HWS–T OPPs. All OPPs were computed for an MV drive system consisting of a squirrel cage IM with 3.45 kV rated voltage, 2.2 kA rated current, 50 Hz nominal frequency, 0.255 p.u. total leakage reactance, and a three-level NPC inverter with a dc-link voltage of $V_{dc} = 4.84$ kV. For demonstration purposes, OPPs with $d = 5$ are used, while the implemented SHE scheme eliminates the 5th, 7th, 11th, and 13th current harmonics. All OPPs are computed assuming $\phi = 35^\circ$, while operation at nominal torque is considered. Additionally, for the torque-constrained OPPs, the weighting matrix is set to $\mathbf{W} = 10^9 \mathbf{I}_2$, with

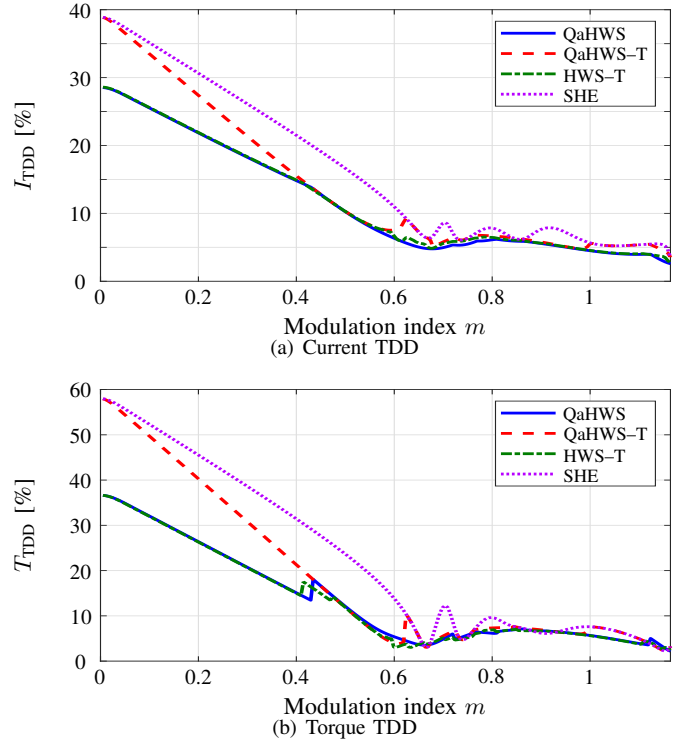


Fig. 3: Programmed modulation methods for $d = 5$ without and with the torque constraint. The solid (blue) line corresponds to conventional QaHWS OPPs, the dashed (red) line to QaHWS–T OPPs, the dash-dotted (green) line to HWS–T OPPs, and the dotted (magenta) line to SHE.

\mathbf{I}_2 denoting the two-dimensional identity matrix. Finally, to ensure full magnetization of the machine, the modulation index is kept proportional to the fundamental frequency, with the nominal modulation index being $m_N = 1.16$ at rated speed.

A. OPPs With Eliminated Low-Order Torque Harmonics

When the nominal modulation index is $m_N = 1.16$, it is physically possible for both QaHWS–T OPPs and SHE to successfully eliminate the n^{th} -order torque harmonic, with $n = 6, 12$, across the whole modulation range of interest, by zeroing the corresponding $n - 1$ and $n + 1$ current harmonics. This, however, leads to a significantly increased current and torque TDD compared to the conventional QaHWS OPPs, see Fig. 3. Moreover, at most modulation indices, SHE results in current distortions higher than or equal to those of the QaHWS–T OPPs, see Fig. 3(a), since it does not explicitly minimize the current distortion. Nevertheless, as observed in Fig. 4(c), both QaHWS–T OPPs and SHE produce the same current and torque harmonics at the nominal modulation index, leading to identical harmonic spectra.

When the symmetry properties of the OPPs are relaxed, the $n - 1$ and $n + 1$ current harmonics only need to have equal (non-zero) amplitudes to eliminate the n^{th} torque harmonic, as illustrated in Fig. 4(e). This enables the elimination of the low-order torque harmonics without significantly affecting the current TDD, see Fig. 3(a). At the nominal modulation index (Fig. 4), the increased I_{TDD} of QaHWS–T OPPs is notably

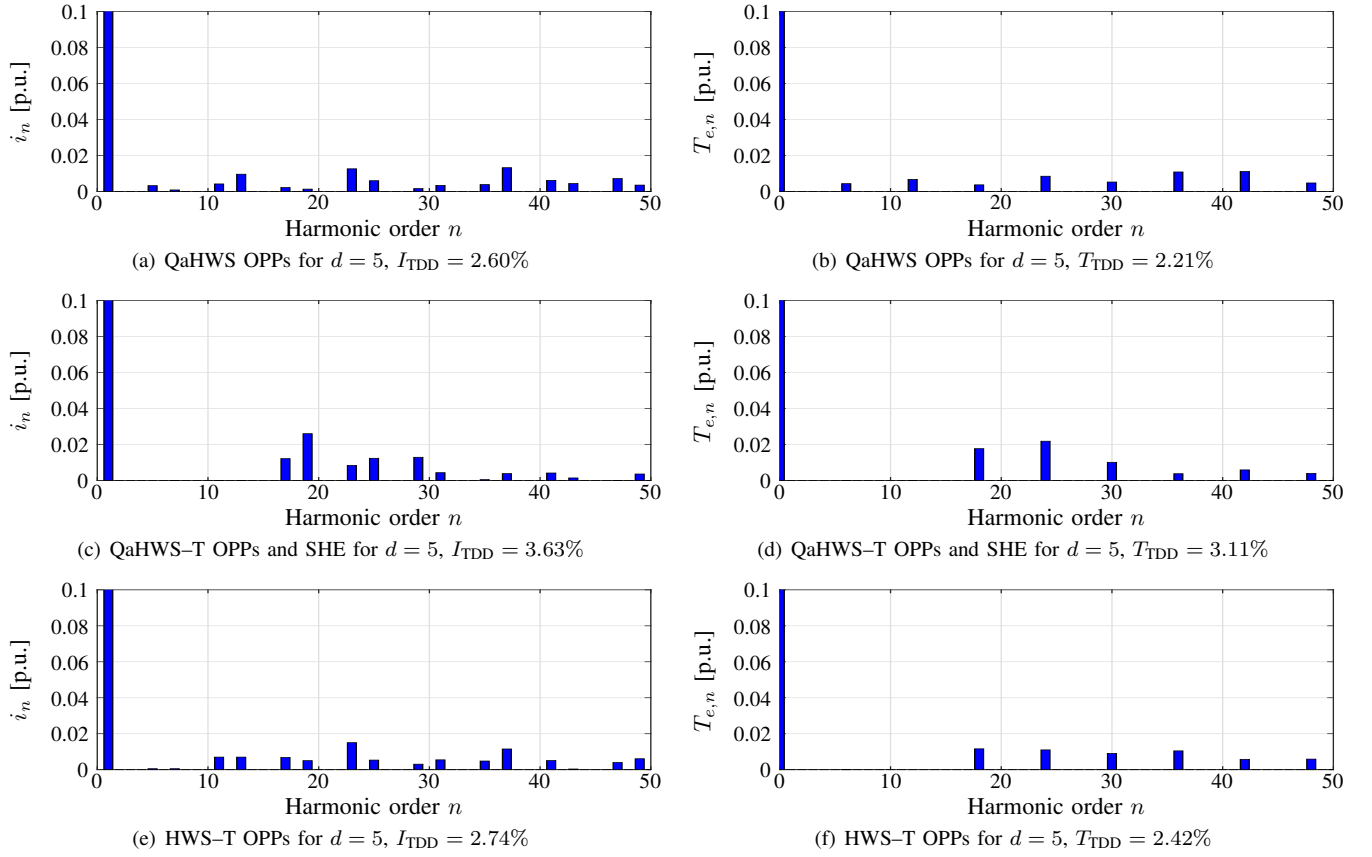


Fig. 4: Current and torque harmonic spectra at modulation index $m = 1.16$.

mitigated by the proposed HWS-T OPPs. Additionally, as a positive byproduct, the torque TDD with HWS-T OPPs remains close to that of conventional QaHWS OPPs, despite this not being an explicit design objective. As seen from Fig. 3(b), there are modulation indices where the proposed HWS-T OPPs not only eliminate the low-order torque harmonics but also improve the torque TDD while keeping the current TDD close to that of conventional QaHWS OPPs.

To visualize this favorable performance, modulation index $m = 0.72$ is considered as an example in Fig. 5. As seen in Fig. 5(c), the low-order current harmonics are zero when QaHWS-T OPPs are used. As a result, the harmonic content shifts to higher frequencies compared to Fig. 5(a), resulting in increased TDD for both the current and torque. In contrast, the proposed HWS-T OPPs successfully eliminate the 6th and 12th torque harmonics while reducing the torque TDD compared to the conventional QaHWS OPPs, see Figs. 5(f) and 5(b). Finally, at this modulation index, SHE performs worse than OPPs both in terms of current and torque distortions.

B. Machine with Higher Rated Voltage

As a special case, we consider an IM with 3.55 kV rated voltage. The total leakage reactance is adjusted to have the same p.u. value used previously. In this scenario, the nominal modulation index becomes $m_N = 1.2$. This section compares

the performance of QaHWS OPPs, QaHWS-T OPPs, HWS-T OPPs, and SHE in terms of current and torque harmonics.

As seen in Fig. 6, SHE finds solutions only up to modulation index $m = 1.17$, which is also the maximum modulation index for which QaHWS-T OPPs can eliminate the 6th and 12th torque harmonics. For higher modulation indices, these harmonics are non-zero with QaHWS-T OPPs. Yet, due to the torque constraints, QaHWS-T OPPs limit the amplitude of the 6th torque harmonic compared to conventional QaHWS OPPs, see Fig. 6(c). This, however, comes at the expense of a slightly increased 12th torque harmonic, see Fig. 6(d).

When the OPP symmetry is relaxed, the low-order torque harmonics can be eliminated without forcing the low-order odd non-triplet current harmonics to zero. As a result, OPPs with zero 6th and 12th torque harmonic can be computed up to modulation index $m = 1.19$. More impressively, this desired feature is achieved without significantly compromising the output current quality, see Fig. 6(a). For modulation indices $m > 1.19$, some low-order torque harmonics appear, but their amplitudes are below 0.01 p.u. and notably lower than those with QaHWS-T OPPs. These reduced torque harmonics, however, come at the cost of increased I_{TDD} compared to QaHWS-T OPPs. Nonetheless, at the nominal modulation, the torque TDD of HWS-T OPPs is lower than that of conventional QaHWS OPPs, see Figs. 7(b) and 7(f). Finally, it should be pointed out that due to the soft constraints, the n^{th}

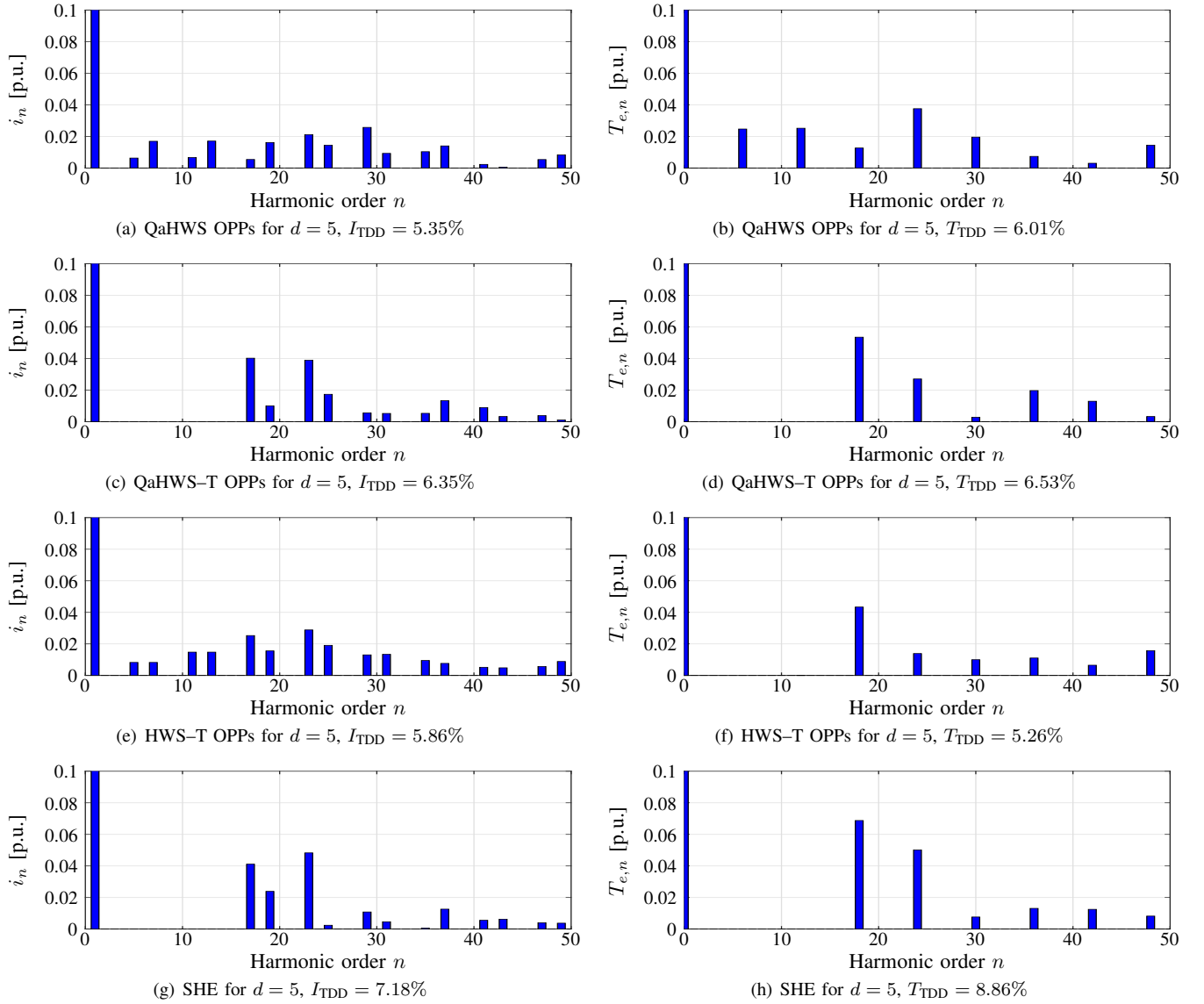


Fig. 5: Current and torque harmonic spectra at modulation index $m = 0.72$.

($n \in \{6, 12\}$) torque harmonic of torque-constrained OPPs is non-zero at the nominal modulation index because the $n-1$ and $n+1$ current harmonics are not equal, see Figs. 7(c) and 7(e).

V. CONCLUSIONS

This paper presented the computation of torque-constrained OPPs, where the—harmful to the machine—low-order torque harmonics are eliminated over the widest physically possible range of modulation indices by directly accounting for them in the OPP optimization problem. At high modulation indices, where complete elimination is not feasible, these harmonics are minimized as much as possible. Moreover, as demonstrated by the presented numerical results, relaxing artificial symmetry restrictions in the OPPs enables this desirable behavior without significantly compromising the current and torque TDD over a

wider range of operating points, thereby preventing an increase in the machine losses.

APPENDIX

Assuming QaHWS, (12) is simplified to

$$T_{e,n} = \frac{V_{dc}}{2\omega_1 \text{pf}} \left(\left(\left(I_1 \sin \phi - \frac{1}{X_\sigma} \right) \left(\frac{b_{n-1}}{n-1} - \frac{b_{n+1}}{n+1} \right) \right)^2 + \left(I_1 \cos \phi \left(\frac{b_{n-1}}{n-1} + \frac{b_{n+1}}{n+1} \right) \right)^2 \right)^{\frac{1}{2}}. \quad (17)$$

Therefore, to eliminate the n^{th} torque harmonic, the following conditions should hold

$$\begin{cases} \left(I_1 \sin \phi - \frac{1}{X_\sigma} \right) \left(\frac{b_{n-1}}{n-1} - \frac{b_{n+1}}{n+1} \right) = 0 & \text{and} \\ I_1 \cos \phi \left(\frac{b_{n-1}}{n-1} + \frac{b_{n+1}}{n+1} \right) = 0 \end{cases} \quad (18)$$

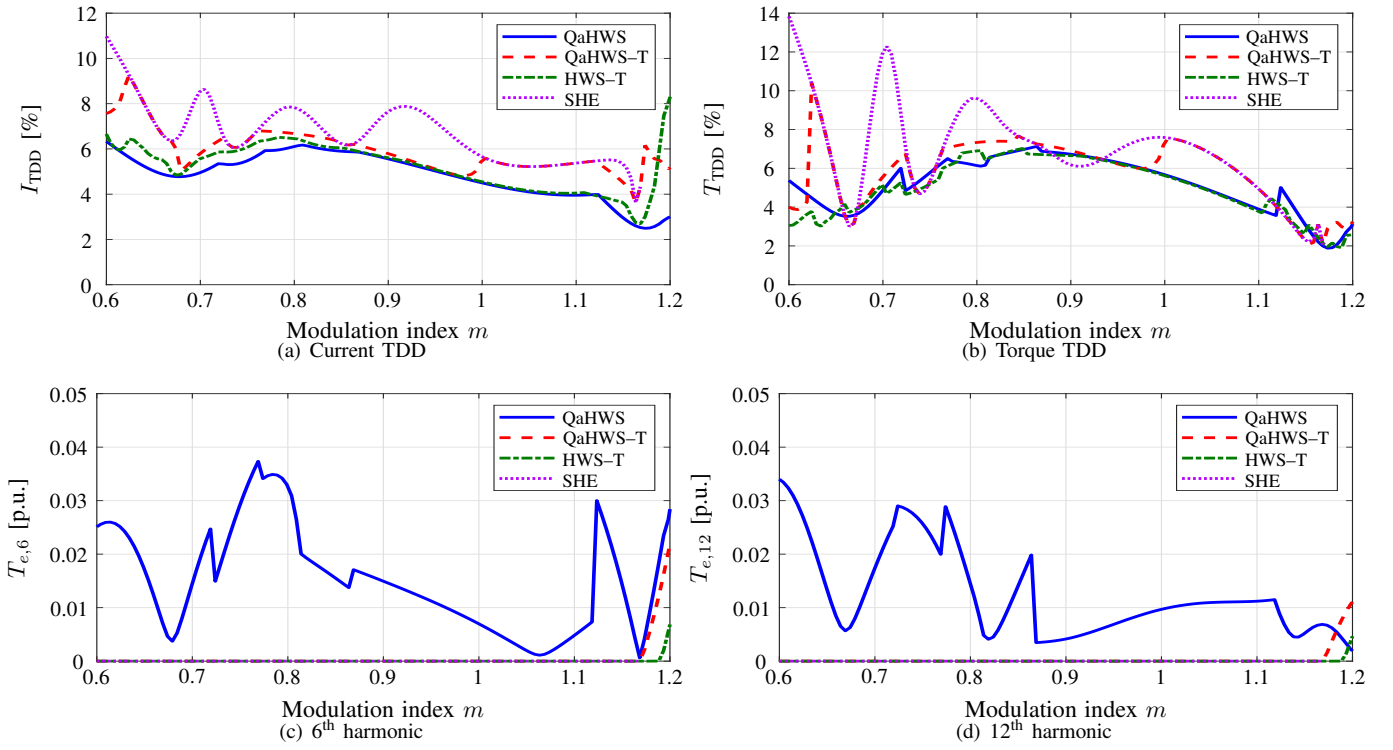


Fig. 6: Programmed modulation methods for $d = 5$ without and with the torque constraint. The solid (blue) line corresponds to conventional QaHWS OPPs, the dashed (red) line to QaHWS-T OPPs, the dash-dotted (green) line to HWS-T OPPs, and the dotted (magenta) line to SHE.

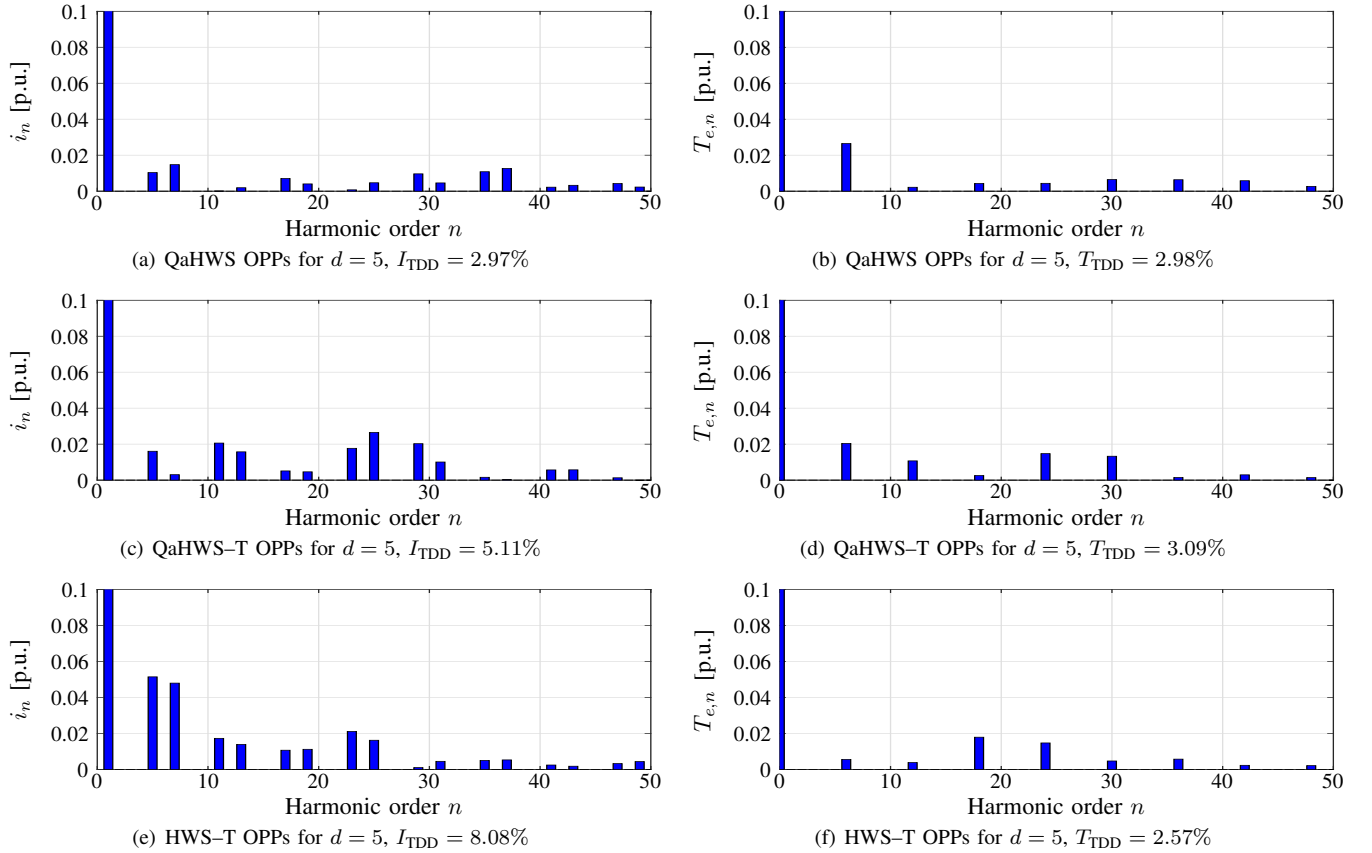


Fig. 7: Current and torque harmonic spectra at modulation index $m = 1.2$.

These conditions result in

$$\frac{b_{n-1}}{n-1} = \frac{b_{n+1}}{n+1} = 0, \quad (19)$$

which implies that

$$\hat{i}_{n-1} = \hat{i}_{n+1} = 0.$$

Assuming HWS, to achieve $T_{e,n} = 0$, the following should hold

$$\begin{cases} \left(I_1 \sin \phi - \frac{1}{X_\sigma} \right) \left(\frac{b_{n-1}}{n-1} - \frac{b_{n+1}}{n+1} \right) - I_1 \cos \phi \left(\frac{a_{n-1}}{n-1} + \frac{a_{n+1}}{n+1} \right) = 0 \\ \left(I_1 \sin \phi - \frac{1}{X_\sigma} \right) \left(\frac{a_{n-1}}{n-1} - \frac{a_{n+1}}{n+1} \right) + I_1 \cos \phi \left(\frac{b_{n-1}}{n-1} + \frac{b_{n+1}}{n+1} \right) = 0 \end{cases} \quad (20)$$

Expression (20) corresponds to a system of two equations with four unknowns. Therefore, a_{n-1} and b_{n-1} can be expressed as a function of a_{n+1} and b_{n+1} according to

$$\frac{a_{n-1}}{n-1} = \frac{\left(I_1 \sin \phi - \frac{1}{X_\sigma} \right)^2 - (I_1 \cos \phi)^2 a_{n+1} + \frac{-2 \left(I_1 \sin \phi - \frac{1}{X_\sigma} \right) (I_1 \cos \phi) b_{n+1}}{\left(I_1 \sin \phi - \frac{1}{X_\sigma} \right)^2 + (I_1 \cos \phi)^2 n + 1}}{\left(I_1 \sin \phi - \frac{1}{X_\sigma} \right)^2 + (I_1 \cos \phi)^2 n + 1}} \quad (21a)$$

$$\frac{b_{n-1}}{n-1} = \frac{2 \left(I_1 \sin \phi - \frac{1}{X_\sigma} \right) (I_1 \cos \phi) a_{n+1} + \frac{\left(I_1 \sin \phi - \frac{1}{X_\sigma} \right)^2 - (I_1 \cos \phi)^2 b_{n+1}}{\left(I_1 \sin \phi - \frac{1}{X_\sigma} \right)^2 + (I_1 \cos \phi)^2 n + 1}}{\left(I_1 \sin \phi - \frac{1}{X_\sigma} \right)^2 + (I_1 \cos \phi)^2 n + 1}} \quad (21b)$$

Based on the above, the following relationships should hold

$$\left(\frac{a_{n-1}}{n-1} \right)^2 + \left(\frac{b_{n-1}}{n-1} \right)^2 = \left(\frac{a_{n+1}}{n+1} \right)^2 + \left(\frac{b_{n+1}}{n+1} \right)^2 \quad (22a)$$

$$\text{atan} \frac{a_{n-1}}{b_{n-1}} - \text{atan} \frac{a_{n+1}}{b_{n+1}} = \text{atan} \frac{2 \left(\frac{1}{X_\sigma} - I_1 \sin \phi \right) (I_1 \cos \phi)}{\left(I_1 \sin \phi - \frac{1}{X_\sigma} \right)^2 - (I_1 \cos \phi)^2}. \quad (22b)$$

Condition (22a) implies that

$$\hat{i}_{n-1} = \hat{i}_{n+1},$$

while condition (22b) implies that

$$\angle \hat{i}_{n+1} - \angle \hat{i}_{n-1} = \text{atan} \frac{2 \left(\frac{1}{X_\sigma} - I_1 \sin \phi \right) (I_1 \cos \phi)}{\left(I_1 \sin \phi - \frac{1}{X_\sigma} \right)^2 - (I_1 \cos \phi)^2}.$$

ACKNOWLEDGMENT

This work was supported in part by ABB Oy Drives and in part by the Research Council of Finland.

REFERENCES

- [1] H. S. Patel and R. G. Hoft, "Generalized techniques of harmonic elimination and voltage control in thyristor inverters: Part I—harmonic elimination," *IEEE Trans. Ind. Appl.*, vol. IA-9, no. 3, pp. 310–317, May/Jun. 1973.
- [2] —, "Generalized techniques of harmonic elimination and voltage control in thyristor inverters: Part II — voltage control techniques," *IEEE Trans. Ind. Appl.*, vol. IA-10, no. 5, pp. 666–673, Sep./Oct. 1974.
- [3] G. S. Buja and G. B. Indri, "Optimal pulsewidth modulation for feeding ac motors," *IEEE Trans. Ind. Appl.*, vol. IA-13, no. 1, pp. 38–44, Jan./Feb. 1977.
- [4] J. Song-Manguelle, S. Schröder, T. Geyer, G. Ekemb, and J.-M. Nyobe-Yome, "Prediction of mechanical shaft failures due to pulsating torques of variable-frequency drives," *IEEE Trans. Ind. Appl.*, vol. 46, no. 5, pp. 1979–1988, Sep./Oct. 2010.
- [5] J. Song-Manguelle, J.-M. Nyobe-Yome, and G. Ekemb, "Pulsating torques in PWM multi-megawatt drives for torsional analysis of large shafts," *IEEE Trans. Ind. Appl.*, vol. 46, no. 1, pp. 130–138, Jan./Feb. 2010.
- [6] Y. Plotkin, M. Stiebler, and D. Hofmeyer, "Sixth torque harmonic in PWM inverter-fed induction drives and its compensation," *IEEE Trans. Ind. Appl.*, vol. 41, no. 4, pp. 1067–1074, Jul./Aug. 2005.
- [7] N. Nakao and K. Akatsu, "Suppressing pulsating torques: Torque ripple control for synchronous motors," *IEEE Ind. Appl. Mag.*, vol. 20, no. 6, pp. 33–44, Nov./Dec. 2014.
- [8] V. S. S. Pavan Kumar Hari and G. Narayanan, "Space-vector-based hybrid PWM technique to reduce peak-to-peak torque ripple in induction motor drives," *IEEE Trans. Ind. Appl.*, vol. 52, no. 2, pp. 1489–1499, Mar./Apr. 2016.
- [9] H.-S. Jung, C.-E. Hwang, H.-S. Kim, S.-K. Sul, A. Hee-Won, and H. Yoo, "Minimum torque ripple pulse width modulation with reduced switching frequency for medium-voltage motor drive," *IEEE Trans. Ind. Appl.*, vol. 54, no. 4, pp. 3315–3325, Jul./Aug. 2018.
- [10] J. M. D. Murphy and M. G. Egan, "A comparison of PWM strategies for inverter-fed induction motors," *IEEE Trans. Ind. Appl.*, vol. IA-19, no. 3, pp. 363–369, May/Jun. 1983.
- [11] C. Feng, P. Wang, S. Huang, Z. Zhang, W. Liao, G. Liang, Y. Liu, X. Wu, and S. Huang, "A novel torque harmonics suppression PWM method of high-speed PMSG for microturbine power generation system," *IEEE Trans. Transp. Electr.*, vol. 10, no. 3, pp. 7275–7285, Sep. 2024.
- [12] Z. Shao, Z. Ma, J. Gong, and Y. Peng, "Torque ripple suppression synchronous optimal PWM for IPMSMs by reallocating current harmonics in multiple synchronous reference frame," *IEEE Trans. Power Electron.*, vol. 40, no. 8, pp. 11 775–11 786, Aug. 2025.
- [13] A. Tripathi and G. Narayanan, "Torque ripple minimization in neutral-point-clamped three-level inverter fed induction motor drives operated at low-switching-frequency," *IEEE Trans. Ind. Appl.*, vol. 54, no. 3, pp. 2370–2380, May/Jun. 2018.
- [14] —, "Analytical evaluation and reduction of torque harmonics in induction motor drives operated at low pulse numbers," *IEEE Trans. Ind. Electron.*, vol. 66, no. 2, pp. 967–976, Feb. 2019.
- [15] S. Yadav, S. K. Mallik, and A. Mishra, "Optimal harmonic mitigation technique for high-power IM drives," *Electr. Eng.*, vol. 107, no. 1, pp. 853–867, Jan. 2025.
- [16] Y. Shen, Y. Ma, Y. Zhang, Z. Yin, and H. Zhao, "An improved torque ripple minimization pulsewidth modulation for induction motors under low carrier ratio," in *Proc. Inter. Conf. Electr. Mach. Syst.*, Fukuoka, Japan, Nov. 2024, pp. 2787–2791.
- [17] E. Kontodinas, P. Karamanakos, A. Kraemer, and S. Wendel, "Optimized pulse patterns for anisotropic synchronous machines with improved current and torque properties," in *Proc. Eur. Conf. on Power Electron. and Applicat.*, Aalborg, Denmark, Sep. 2023, pp. 1–8.
- [18] M. Gu, Z. Wang, and B. Wang, "Optimization of torque ripple for low-carrier-ratio dual three-phase PMSM with pulse pattern control," *IEEE Trans. Power Electron.*, vol. 38, no. 12, pp. 15 091–15 096, Dec. 2023.
- [19] G. Liang, S. Huang, W. Liao, Z. Zhang, Y. Liu, C. Feng, X. Wu, and S. Huang, "An optimized modulation of torque and current harmonics suppression for dual three-phase PMSM," *IEEE Trans. Transp. Electr.*, vol. 10, no. 2, pp. 3443–3454, Jun. 2024.
- [20] A. Birth, T. Geyer, H. d. T. Mouton, and M. Dorfling, "Generalized three-level optimal pulse patterns with lower harmonic distortion," *IEEE Trans. Power Electron.*, vol. 35, no. 6, pp. 5741–5752, Jun. 2020.